n

Plancq, J., Mattioli, E., Pittet, B., Baudin, F., Duarte, L.V., Boussaha, M., and Grossi, V. (2016) A calcareous nannofossil and organic geochemical study of marine palaeoenvironmental changes across the Sinemurian/Pliensbachian (early Jurassic, ~191Ma) in Portugal. Palaeogeography, Palaeoclimatology, Palaeoecology, 449, pp. 1-12.

There may be differences between this version and the published version. You are advised to consult the publisher's version if you wish to cite from it.

http://eprints.gla.ac.uk/116929/

Deposited on: 04 March 2016

Enlighten – Research publications by members of the University of Glasgow
http://eprints.gla.ac.uk

*Revision with No Changes Marked
Click here to view linked References

A calcareous nannofossil and organic geochemical study of marine palaeoenvironmental changes across the Sinemurian/Pliensbachian (early Jurassic, ~191 Ma) in Portugal

J. Plancq[a, b*], E. Mattioli[a], B. Pittet[a], F. Baudin[c], L.V. Duarte[d], M. Boussaha[e], V. Grossi[a]

[a] Univ Lyon, Université Claude Bernard Lyon 1, ENS de Lyon, CNRS, UMR 5276 LGL-TPE, F-69622, Villeurbanne, France.

[b] Present address: School of Geographical and Earth Sciences, University of Glasgow, Glasgow G12 8QQ, UK.

[c] Sorbonne Universités, UPMC Université Paris 06, UMR 7193, ISTeP, 75005 Paris, France.

[d] MARE-Marine and Environmental Sciences Centre, Faculty of Sciences and Technology, Department of Earth Sciences, University of Coimbra, Rua Sílvio Lima, 3030-790 Coimbra, Portugal.

[e] Department of Geosciences and Natural Resource Management, University of Copenhagen, Øster Voldgade 10, 1350 Copenhagen, Denmark

[*] Corresponding author: School of Geographical and Earth Sciences, University of Glasgow, Office number 421, Gregory Building, Lilybank Gardens, Glasgow G12 8QQ, UK. Email address: julien.plancq@glasgow.ac.uk; Tel: +44 (0)141 330 5449.

Email addresses: julien.plancq@glasgow.ac.uk (J. Plancq), emanuela.mattioli@univ-lyon1.fr (E. Mattioli), bernard.pittet@univ-lyon1.fr (B. Pittet), francois.baudin@upmc.fr (F. Baudin), lduarte@dct.uc.pt (L.V. Duarte), myriam.boussaha@ign.ku.dk (M. Boussaha), vincent.grossi@univ-lyon1.fr (V. Grossi).

Abstract

The Sinemurian/Pliensbachian boundary (~191 Ma) is acknowledged as one of the most important steps in the radiation of planktonic organisms, especially primary producers such as dinoflagellates and coccolithophores. To date, there is no detailed study documenting changes in planktonic assemblages related to palaeoceanographic changes across this boundary. The aim of this study is to characterize the palaeoenvironmental changes occurring across the Sinemurian/Pliensbachian boundary at the São Pedro de Moel section (Lusitanian Basin, Portugal) using micropalaeontology and organic geochemistry approaches. Combined calcareous nannofossil assemblage and lipid biomarker data document for a decrease in primary productivity in relation to a major sea-level rise occurring above the boundary. The Lusitanian Basin was particularly restricted during the late Sinemurian with a relatively low sea level, a configuration that led to the recurrent development of black shales. After a sharp sea-level fall, the basin became progressively deeper and more open during the earliest Pliensbachian, subsequently to a major transgression. This sea-level increase seems to have been a global feature and could be may have been related to the opening of the Hispanic Corridor that connected the Tethys and palaeo-Pacific oceans. The palaeoceanographic and palaeoclimatic changes induced by this opening may have played a role in the diversification of coccolithophores with the first occurrence or colonization of Tethyan waters by placolith-type coccoliths.

Keywords: productivity; sea-level; evolutionary events; Hispanic Corridor; coccoliths; lipid biomarkers.

1. Introduction

The early Jurassic is punctuated by episodes of organic matter (OM) deposition and preservation, probably testifying to the sporadic development of dysoxic/anoxic conditions in the epicontinental basins of the western Tethys associated with peculiar tectonic and climatic conditions (e.g., Jenkyns et al., 2002; Rosales et al., 2004; van de Schootbrugge et al., 2005). Amongst them, the Sinemurian/Pliensbachian interval is of particular interest because in some areas like the Lusitanian (Portugal), Basque-Cantabrian (Spain) and Bristol Channel and Wessex (England) basins, laminated OM-rich levels (black shales) are characterized by a very high (up to 20%) total organic carbon (TOC) content (Jenkyns et al., 2002; Deconinck et al., 2003; Rosales et al., 2004; Van de Schootbrugge et al., 2005; Duarte et al., 2010). In the Lusitanian Basin, the richness in organic matter makes the late Sinemurian-early Pliensbachian one of the most important intervals of potential oil source rocks (e.g., Duarte et al., 2010, 2012; Silva et al. 2013).

The Sinemurian/Pliensbachian boundary (~191 Ma) has been well documented for its macroinvertebrate record (e.g., Mouterde, 1967; Antunes et al., 1981; Dommergues and El Hariri, 2002; Meister et al., 2012; Comas-Rengifo et al., 2013; Duarte et al., 2014), and a precise stratigraphic framework has allowed definition of the Global Stratotype Section and Point (GSSP) of the Pliensbachian Stage at Wine Haven, Yorkshire (Meister et al., 2006). This time interval is also recognized as one of the most important steps in the radiation of planktonic organisms, especially primary producers such as dinoflagellates (van de

Schootbrugge et al., 2005) and coccolithophores (Bown et al., 2004). It is around this boundary that first occurred the placolith coccolith-type (for example *Similiscutum*), which marks an important event in the diversification history of the coccolithophores. This radiation is probably linked to major palaeoceanographic changes related to the opening of the Hispanic Corridor described by some authors (van de Schootbrugge et al., 2005; Dera et al., 2015). A negative excursion in the carbon isotopic composition ($\delta^{13}C$) in carbonates has been recorded in the Cleveland Basin (England) and interpreted as a major perturbation in the carbon cycle (e.g., Jenkyns et al., 2002; Korte and Hesselbo, 2011). In spite of this, there is no detailed study documenting changes in planktonic assemblages across the Sinemurian/Pliensbachian boundary, while the palaeoceanographic and/or productivity changes occurring at that time are poorly understood. In addition, only few studies have provided isotopic data for the Sinemurian/Pliensbachian, and the main features and causes of the $\delta^{13}C$ excursion remain unclear (e.g., Hesselbo et al., 2000; Jenkyns et al., 2002; Duarte et al., 2014).

The aim of this study is thus to appraise the palaeoenvironmental changes occurring across the Sinemurian/Pliensbachian boundary at the São Pedro de Moel section (Lusitanian Basin, Portugal) using micropalaeontology and organic geochemistry approaches at high resolution, and to relate these changes to the palaeoceanographic events characterizing the western Tethys in the early Jurassic. Sedimentological analyses combined to bulk organic matter characterization, calcareous nannofossil quantification, and lipid biomarker analysis allow for the first time discussing the changes in primary productivity, the major evolutionary events and their links with sea-level changes in Sinemurian/Pliensbachian sediments.

2. Geological setting

The composite São Pedro de Moel section comprises the sections of Água de Madeiros (39°44′27″ N; 9°02′20″ W) and Polvoeira-Pedra do Ouro (39°43′18″ N; 9°02′56″ W) and outcrops along the coastline of central-western Portugal, approximately 110 km north of Lisbon (Duarte and Soares, 2002; Duarte et al., 2012) (Fig. 1a). This locality was palaeogeographically located in the central-western part of the Lusitanian Basin. In the Jurassic, this narrow and north-south elongated basin developed at the western margin of the Tethys Ocean, and resulted from the aborted rifting of the proto-Atlantic (Manspeizer, 1988; Soares et al., 1993). The Lusitanian Basin was bounded to the East by the Iberian Meseta and to the West by the Variscan (granitic and metamorphic) Berlenga-Farilhões Horst (Fig. 1b and c). The Lusitanian Basin was connected to the north-western European epicontinental basins and to the Hispanic Corridor to the south, thus representing a key location between the proto-Atlantic and Tethyan oceanic domains (Fig. 1b). The peculiar setting of São Pedro de Moel in the central deepest part of the basin accounts for the completeness of the upper Sinemurian-lower Pliensbachian sedimentary record in a relatively expanded 58 m-thick section. Numerous ammonite and calcareous nannofossil bioevents are recorded in this section, providing a detailed biostratigraphic framework (e.g. Mouterde, 1967; Antunes et al., 1981; Meister et al., 2012; Comas-Rengifo et al., 2013; Mattioli et al., 2013; Duarte et al., 2014; Boussaha et al., 2014). The studied time interval includes the Ammonite Oxynotum, Raricostatum and Jamesoni Zones and the Nannofossil NJT 3a, NJT 3b and NJT 4 Zones (Fig. 2).

In the upper Sinemurian/lower Pliensbachian, the sedimentation was characterized by marl-limestone alternations with common occurrence of black shales (organic carbon-rich sedimentary levels), belonging to the Água de Madeiros and Vale das Fontes formations. The Água de Madeiros Formation can be subdivided into the Polvoeira and Praia da Pedra Lisa members (Duarte and Soares, 2002; Duarte et al., 2004, 2010; Duarte, 2007). Interpretation of

the depositional environments of the São Pedro de Moel section and its sequence stratigraphical evolution have been presented by Boussaha et al. (2014) and are summarized in Figure 2. Briefly, the first 42 meters of the section are characterized by a 2nd-order transgression (see Duarte et al., 2010) indicated by facies evolution from mid to outer-ramp environments. Black shales interbedded with storm deposits are frequently recorded in this interval. Above, the facies succession suggests an evolution from outer to mid-to-inner-ramp, attesting for a major sea-level fall. The lowest sea level is recorded between 55 and 62 meters with a sedimentation dominated by amalgamated tempestites that show hummocky cross-stratifications (HCS). The upper part of the section (62-89 m) is characterized by marl-limestone alternations increasingly argillaceous upwards, testifying for a progressive rise in sea level in an outer-ramp environment (Fig. 2).

3. Methods

3.1. Calcareous nannofossils

Eighty-six samples were analysed for calcareous nannofossils, 45 from Pedra do Ouro section and 41 from Água de Madeiros section. Samples were prepared following the technique of Beaufort (1991) modified by Geisen et al. (1999) allowing absolute quantification of nannofossil abundances per gram of rock. Slides were then studied in a ZEISS Axioscope 40 polarising microscope, using a 1000 X magnification. As lower Jurassic nannofossil abundance is low, 250 nannofossils on average (both coccoliths and the *incertae sedis Schizosphaerella* spp. and *Orthogonoides hamiltoniae*) could be counted in each slide. The intervals comprised between 20 and 26 meters (base of the section studied at Pedra do Ouro; Boussaha et al., 2014) and between 62 and 65 meters (after the tempestite interval in Água de Madeiros section) are extremely poor in terms of nannofossil abundance. In these

intervals, total absolute abundances could be calculated but the scarcity of the specimens counted (less than 100) prevented us to confidently calculate the relative abundances of each coccolith taxa. Relative abundance of *Schizosphaerella* spp. and *Orthogonoides hamiltoniae* were calculated with respect to the total nannofossil abundance for 86 samples, while species-specific relative abundances of the coccolith species were calculated with respect to the counted coccolith number for the 49 richest samples.

Nannofossil preservation was also evaluated in each sample by taking into account the degree of etching and overgrowth according to Roth (1984), as well as the degree of fragmentation. Three classes of preservation were thus used: poor for nannofossil assemblages showing strong etching, overgrowth or fragmentation, moderate for moderate etching, overgrowth or fragmentation, and good when *Schizosphaerella* spp. Fragmentation was limited or absent and delicate coccoliths displayed relatively pristine structures.

3.2. Rock-Eval pyrolysis

In order to obtain information on the type and thermal maturity of the bulk OM, Rock-Eval analyses were performed on 23 samples with a Rock-Eval device (Vinci Technologies) under standard conditions (see all details about Rock-Eval pyrolysis and parameters in Espitalié, 1993; Behar et al., 2001). Measurements made include S_1 (mg HC/g rock), S_2 (mg HC/g rock), S_3 (mg CO_2/g rock) and T_{max} (°C). Derived parameters such as the Total Organic Carbon (TOC) content (wt.%), the Hydrogen Index (HI = S_2/TOCx100; mg HC/g TOC) and the Oxygen Index (OI= S_3/TOCx100; mg CO_2/g TOC) were also determined.

3.3. Lipid biomarkers

From the 23 samples used for Rock-Eval analyses, 19 organic matter-rich marls were selected and studied for their aliphatic hydrocarbon composition. Samples (ca. ~30 g) were

ground and Soxhlet-extracted during 16 hours with Dichloromethane (DCM)/Methanol (MeOH) (7:1 v/v). Total lipid extracts were concentrated and diluted in a Heptane/DCM (40:1 v/v) solution in order to precipitate asphaltenes. Maltene extracts were then fractionated into five fractions by liquid chromatography over a wet packed column of inactivated (4% H_2O) silica. Aliphatic hydrocarbons were eluted with *n*-hexane, aromatic hydrocarbons with hexane:DCM (4:1 v/v), ketones with toluene, alcohols with hexane-ethyl acetate (9:1 v/v), and polars with DCM-methanol (1:1 v/v). Aliphatic hydrocarbons were then dried under a stream of nitrogen, and a known amount of squalane was added as an internal standard before analysis by gas chromatography (GC/FID) and gas chromatography/mass spectrometry (GC/MS).

Hydrocarbons were identified using a MD800 Voyager spectrometer interfaced to an HP6890 gas chromatograph equipped with an on-column injector and a DB-5MS column (30 m x 0.25 mm x 0.25 µm). The oven temperature was programmed from 60°C (1 min) to 130°C at 20°C min^{-1}, and then to 310°C (20 min) at 4°C min^{-1}. Helium was used as the carrier gas at constant flow (1 $mL.min^{-1}$). Selective detection of hopanes and steranes was realized by ion extraction (191 and 217, respectively).

Compound abundances were determined by GC/FID using a HP6890 Series gas chromatograph configured as for GC-MS analyses.

3.4. Biomarkers used in this study

To better characterize changes in primary productivity, we have selected some biomarkers to be analysed. These are:

(1) Phytane, a chlorophyll-derived (phytol) biomarker that can be used as an indicator of primary productivity (Didyk et al., 1978);

(2) Sterols, produced by eukaryotic algae, protists and multicellular eukaryotes (Volkman et al., 1998). Algae and metazoa are the main producers of C_{27} sterols, whereas C_{28} sterols are associated with chlorophyll *c*-containing phytoplankton such as diatoms, dinoflagellates and coccolithophores (Knoll et al., 2007). C_{29} sterols are mostly attributed to higher land plants (Volkman et al., 1998) although contribution from marine green algae (Knoll et al., 2007) or freshwater microalgae (Volkman et al., 1999; Kodner et al., 2008) is also possible. Therefore, secular variations of different groups of steranes can be interpreted in terms of ecological successions among groups of organisms and/or varying terrestrial inputs to the sediments;

(3) C_{27}-C_{35} hopanes, derived from C_{35} bacteriohopanepolyols synthesized by some members of the Bacteria including cyanobacteria (Rohmer et al., 1984; Ourisson et al., 1987). The proportions of regular C_{27-29} steranes relative to C_{30-35} hopanes, here expressed as St/(St+Hop) ratio, can be used for estimating the relative input of eukaryotic (mostly algae and/or higher plants) and bacterial biomass to sediments (Peters et al., 2005).

3.5. Isotope analyses

In order to measure their organic carbon isotopic composition ($\delta^{13}C_{TOC}$), aliquots of the 19 marl samples studied for their aliphatic hydrocarbon composition were decarbonated using 2N HCl for 24h at ambient temperature. They were then rinsed with deionized water, centrifuged, rinsed again until neutrality and dried in an oven at 60°C. About 0.2 mg of decarbonated sample were weighed in tin capsules and placed in a Eurovector Elemental Analyzer (EuroEA3028-HT) connected to a GV instrument Isoprime^{TM} stable isotope-ratio mass spectrometer. The stable carbon isotope ratios are reported in the delta notation as the per mil (‰) deviation relative to the Vienna Pee Dee belemnite (V-PDB) standard. Analytical precision and accuracy were determined by triplicate analyses and by comparison with international (IAEA CH7; $\delta^{13}C$= -28.73‰) and in-house (TPAC, Phenyl/Amine; $\delta^{13}C$= -

32.15‰) standards, which were analysed continuously throughout the generation of each isotopic data set. Reproducibility was better than 0.1 ‰ for $\delta^{13}C_{TOC}$ values.

Finally, the carbon isotopic composition of carbonates ($\delta^{13}C_{carb}$) was determined for samples A to N and SPM-OU, by using an auto sampler Multiprep coupled to a Dual-Inlet GV-Isoprime^{TM} mass spectrometer. For each sample, an aliquot of calcium carbonate (between 1150 and 500 µg according to the initial carbonate calcium content of the sample) was reacted with anhydrous oversaturated phosphoric acid at 90°C during 20 min. Isotope values are quoted in the delta notation in per mil relative to V-PDB. Each sample analysis was duplicated and adjusted to the international reference NIST NBS19 ($\delta^{13}C$= +1.95‰). Reproducibility was 0.03 ‰ for $\delta^{13}C_{carb}$ values.

4. Results

4.1. Calcareous nannofossils

Nannofossil preservation is generally moderate to good in the São Pedro de Moel composite section, with fragile structures such as the long and delicate spines of *Parhabdolithus liasicus liasicus* commonly observed.

Nannofossil absolute abundances (both coccoliths and nannoliths) greatly fluctuated in the studied interval (Fig. 3). On the long-term trend, very low values (<10*10^6 nannofossils/g of sediment) are recorded in the Oxynotum Ammonite Zone, but an increase up to 275*10^6 nannofossils/g of sediment is observed in the Raricostatum Ammonite Zone reaching the highest values around the maximum flooding surface (MFS) (Fig. 3). This is followed by a decrease to very low values in the base of the Jamesoni Zone (including the interval dominated by the HCS-bearing tempestites) where a forced regression (FR) occurred. Absolute abundance progressively rises again up to 180*10^6 nannofossils/g of sediment

afterwards, but never reaches again the high values observed around the MFS in the Raricostatum Zone. At a higher frequency, fluctuations are observed in link with lithology, namely higher values are recorded in marly intervals and lower values in limestones (Fig. 3).

Nannofossil assemblages are dominated by *Schizosphaerella* spp. in most of the studied interval, as testified by its very high proportions (between 75 and 100%) in the Oxynotum and Raricostatum Zones, except at the transition between these two zones where percentages drop down to ~25% (Fig. 3). In the Jamesoni Zone, *Schizosphaerella* spp. percentages tend to decrease especially in the upper part of the composite section. Fluctuations at a higher frequency are also observed in link with lithology, but contrary to nannofossil absolute abundances, higher values of *Schizosphaerella* relative abundances are recorded in limestones and lower values in marly intervals (Fig. 3).

The coccolith assemblages are mainly represented by the species *Parhabdolithus liasicus distinctus*, *Parhabdolithus liasicus liasicus*, *Parhabdolithus robustus, Tubirhabdus patulus, Crucirhabdus primulus*, *Crepidolithus pliensbachensis*, *Crepidolithus crassus*, *Mitrolithus lenticularis*, *Mitrolithus jansae*, and *Mitrolithus elegans*. Some taxa, namely *P. liasicus liasicus*, *T. patulus*, and *C. pliensbachensis*, show a trend similar to that of nannofossil absolute abundances (Fig. 3). On the contrary, *P. liasicus distinctus* shows an opposite trend, with lowest relative abundances recorded when nannofossil absolute abundance values are at the highest (Fig. 3). *M. jansae* and *M. elegans* peak in few peculiar intervals in some OM-rich layers deposited above storm events and after the HCS-bearing tempestite interval (62-70 m; Fig. 3).

4.2. TOC and Rock-Eval pyrolysis

The studied samples are characterized by relatively high TOC content (4.5 wt.% on average). Higher values are recorded in the Raricostatum Zone and a trend to decreasing values, from 5.8 to 3.3 wt.%, is observed towards the Jamesoni Zone (Fig. 4).

Rock-Eval S_1 and S_2 parameters vary between 0.09 and 1.41 mg HC/g rock and between 4.25 and 42.77 mg HC/g rock, respectively. The HI and OI values range from 154 to 561 mg HC/g TOC and from 23 to 86 mg CO_2/g TOC, respectively. T_{max} values vary between 417 and 437°C, with an average of 426°C. The crossplot of HI/T_{max} indicates that OM is immature and has undergone only minor thermal diagenesis (Fig. 5). The OM is of Type II and thus dominantly of marine origin, as shown by the plot HI versus OI data (Fig. 5). A general increase of OI is noted with decreasing HI and TOC, suggesting that, for some samples, the marine organic matter suffered a slight oxidation at the time of its deposition.

All these results are consistent with those presented by Duarte et al. (2012) and Poças Ribeiro et al. (2013), who studied the palynofacies and the organic geochemistry (TOC content, Rock-Eval pyrolysis) of the São Pedro de Moel composite section at a higher resolution.

4.3. Lipid biomarkers

The presence of biodegradable short chain *n*-alkanes and acyclic isoprenoids such as pristane (Pr) and phytane (Ph) suggests slight to moderate levels of biodegradation of the OM present in the samples (Peters et al., 2005). This implies that more resistant biomarkers such as regular C_{27-29} steranes and C_{29}-C_{32} hopanes used in this study have not been severely affected by biodegradation.

The concentration in phytane shows a decreasing trend, with a mean phytane content of 105 µg/gTOC to 39 µg/gTOC from the Raricostatum to the Jamesoni Zone (Fig. 4).

295 The Steranes/Hopanes ratio (St/(St+Hop)) is low (<1) throughout the entire studied interval
296 but a decreasing trend is observed (from 0.44 to 0.32), especially in the Jamesoni Zone above
297 the HCS-bearing tempestite interval (Fig. 4).

298 The C_{27} (marine plankton), C_{28} (chlorophyll-c phytoplankton) and, especially, C_{29} (mostly
299 higher land plants) sterane concentrations show the same trend across the studied interval: an
300 increase through the Raricostatum and Jamesoni Zones with a peak at the top of the HCS-
301 bearing interval, followed by a decrease during the transgressive trend of the Jamesoni Zone
302 (Fig. 4). Through the whole studied interval, C_{29} steranes show higher concentrations (17 µg/g
303 TOC) compared to C_{27} (7 µg/g TOC) and C28 steranes (4 µg/g TOC), with a much
304 pronounced peak concentration following the tempestite interval. The sum of hopanes shows
305 an increasing trend throughout the studied interval, rising from 36 µg/gTOC in the
306 Rariscotatum Zone to 90 µg/gTOC in the Jamesoni Zone (Fig. 4).

307

308 *4.4. Carbon isotopes*

309 The $\delta^{13}C_{carb}$ values vary between -1.59‰ and +1.21‰ (Fig. 4). A negative shift of ~2‰ is
310 observed around the Sinemurian/Pliensbachian boundary (Raricostatum/Jamesoni Zones).
311 Our results are similar to those presented by Duarte et al. (2014) for the same section and the
312 same time interval.

313 The $\delta^{13}C_{TOC}$ values determined across the studied section vary between -28.16‰ and -
314 29.70‰. Two negative spikes are observed separated by a positive peak occurring at the
315 Sinemurian/Pliensbachian transition (Fig. 4).

316 The $\delta^{13}C_{TOC}$ does not covary with the $\delta^{13}C_{carb}$ and an opposite trend is observed between
317 $\delta^{13}C_{TOC}$ and phytane concentration (R^2 = -0.41; p = 0.0028), with more depleted values (-29.5
318 ‰) recorded when phytane concentration is high (Raricostatum Zone) and less depleted
319 values (-28.5 ‰) for low phytane concentrations (Jamesoni Zone).

5. Discussion

5.1. Changes in sea level and primary production at São Pedro de Moel

Sea-level changes have been described at the São Pedro de Moel composite section in previous sequence stratigraphy studies (Duarte et al., 2010; Boussaha et al., 2014). In the present work, variations in calcareous nannofossil absolute abundances mirror those of the sea level that determined the eco-space available, namely the depth of the photic zone where calcareous phytoplankton could thrive (Fig. 6). This photic zone was reduced in times of low sea level and more expanded in times of transgression or maximum flooding. First, absolute abundance increased after the rapid flooding that occurred in the upper part of the Oxynotum Zone. Values were the highest around the maximum flooding surface of the Raricostatum Zone, and then dropped during the forced regression at the base of the Jamesoni Zone. Finally, abundances rose again progressively after the sequence boundary of the Jamesoni Zone when the sea level progressively increased.

Relative abundances of *Schizosphaerella* spp. also match with these sea-level changes. Mattioli (1997) and Mattioli and Pittet (2004) argued that this nannolith preferentially developed in proximal settings where water mixing during storms favoured the resuspension of the nutrients in surface waters. *Schizosphaerella* spp. has also been reported to present higher percentages in calcareous than in marly lithologies in different early to late Jurassic settings, when oligotrophic conditions occurred both in platform environments and basinal surface waters (e.g., Noël et al., 1994; Bucefalo Palliani et al., 1998; Mattioli and Pittet, 2002; Pittet and Mattioli, 2002). All these observations suggest that this taxon preferentially inhabited proximal settings, and was abundant during periods favourable to carbonate

deposition that commonly corresponded to relative oligotrophic conditions with occasional replenishment in nutrients following storm events.

Variations in abundances of each coccolith species and their link to sea-level changes are more difficult to interpret, since little is known about the ecology of Jurassic taxa. Some taxa, namely *Parhabdolithus liasicus liasicus* and *Tubirhabdus patulus*, seem to be more abundant during maximum flooding or transgressive phases, whereas *P. liasicus distinctus* shows higher relative abundances in the beginning of the transgressive intervals (Fig. 6). The apparent negative correlation between *P. liasicus liasicus* and *P. liasicus distinctus* may be explained by their differences of morphology. Both coccoliths bear spines but *P. liasicus distinctus* is more robust with a shorter spine than *P. liasicus liasicus*, which possesses a very long and thin spine. Although the presence of spines in coccoliths has been linked to protection from zooplankton predation (Young, 1994), the dominance of the long-spined *P. liasicus liasicus* coccoliths may have also increased the buoyancy of the coccosphere in relatively more stratified and distal environments. In an analogous way, long-spined acritarchs (i.e., *Micrhystidium*) are interpreted by some authors as typical of relatively open and distal environments in Jurassic (Bucefalo Palliani et al., 1998) and Holocene (Mudie et al., 2010) series. It is thus likely that *P. liasicus liasicus* was dwelling in a stratified upper photic zone and in relatively distal environments, where it was likely more competitive than *P. liasicus distinctus*.

When looking at variations in TOC and lipid biomarker data, it becomes clear that changes in primary productivity did occur in concert with sea-level changes at the São Pedro de Moel section (Fig. 6). OM preservation may have been enhanced when the basin was the most restricted, a condition that is attained during relatively low sea level in a narrow basin such as the Lusitanian Basin (Boussaha et al., 2014). However, high productivity is also recorded around the maximum flooding interval in the Raricostatum Zone (Fig. 6). This suggests that

OM accumulation was not only favoured by restriction of the basin, but also by peculiar palaeoenvironmental conditions (oceanographic, climatic) triggering high productivity.

Based on the comparison between variations in calcareous nannofossil absolute and relative abundances, in organic matter contents and in biomarker concentrations, five main intervals of varying sea level and primary production can be identified across the studied time interval (Figs. 6 and 7):

(1) The Oxynotum Zone is characterized by very high, although fluctuating, TOC contents (Figs. 4 and 6). OM preservation was particularly effective when the basin was the most restricted, a condition that is attained at the sequence boundary around 20 m. The Lusitanian Basin was then an inner to outer-ramp, with relatively low sea level (Boussaha et al., 2014). Very low nannofossil absolute abundances are recorded in this interval, probably due to a reduced photic zone (Fig. 7).

(2) Calcareous nannofossil absolute abundance increased after the rapid flooding that occurred in the upper part of the Oxynotum Zone and values were the highest around the maximum flooding surface of the Raricostatum Zone, when the photic zone was more expanded thanks to the sea-level increase. High primary production also occurred around this maximum flooding interval, as indicated by high TOC (Duarte et al., 2010; 2012) and phytane concentrations. The St/(St+Hop) ratio further supports this observation, with higher input to sediments of eukaryotic relative to bacterial biomass (Fig. 6).

During this interval, depositional environment was an outer-ramp, and an important contrast is observed between periods during which the water column was well stratified and periods characterized by intense water mixing due to storms (Fig. 7). During storm events, surface waters were replenished in nutrients thus boosting primary production. The eventual water stratification and the respiration of the excess biomass produced during or following storm events regularly led to bottom water dysoxia/anoxia and the formation of black shales.

This was interrupted by temporary re-oxygenation due to storms as indicated by the presence of several distal tempestites and numerous HCSs (Boussaha et al., 2014). The Lusitanian Basin was thus probably under the control of highly variable environmental conditions during the late Sinemurian. Although the mechanisms of these abrupt and frequent environmental changes are unknown, they appear to be linked to climatic variations and to a particular restricted configuration of the Lusitanian Basin, which likely led to the recurrent development of black shales (Boussaha et al., 2014). The interpretation of the water column stratification could be supported by peaks in the relative abundance of *Mitrolithus jansae* (Figs. 3 and 6), considered as a deep-dweller species (Bucefalo Palliani et al., 1998; Mattioli and Pittet, 2004; Tremolada et al., 2005) since its thick coccoliths probably optimized light intensity into the cell by refraction (Mattioli et al., 2008). Mattioli and Pittet (2004) studied calcareous nannofossils from the Umbria-Marche basin (Italy) during the Pliensbachian/Toarcian, and showed that the relative abundance of *M. jansae* tended to increase when the stratification of the water was more pronounced. In the present study, *M. jansae* peaks in a few marly intervals deposited above storm events. This observation suggests that, in the present case, the development of this deep-dweller might have been favoured by the return to water stratification after storm events.

(3) The base of the Jamesoni Zone is marked by a sharp drop in sea level. The following low sea level was characterized by amalgamated HCS-bearing tempestites (Fig. 6). Calcareous nannoplankton probably could not develop under such conditions, as indicated by a drop in absolute abundances (Fig. 6), and basin waters were likely too much oxygenated for OM to be preserved (Fig. 7).

(4) During the basal transgression that followed storm deposits (between 62 and 71 m), contents in TOC and phytane and the St/(St+Hop) ratio indicate that primary productivity progressively decreased (Fig. 6). The concentration peak in C_{29} sterane recorded just above

the HCS interval (Fig. 4) may testify for an input of land plants (Volkman et al., 1998), and thus higher terrestrial input to the sea. Alternatively, this C_{29} sterane peak could result from the contribution of freshwater algae (Volkman et al., 1999; Rodner et al., 2008) induced by freshwater input. However, the contribution of freshwater algae seems unlikely since palynofacies analysis of the São Pedro de Moel section indicates that the OM is mainly of marine origin (Duarte et al., 2012; Poças Ribeiro et al., 2013). In addition, an episode of strong continental contribution is reflected by an increase in phytoclast content just above the HCS interval (Poças Ribeiro et al., 2013). Thus, the C_{29} sterane content rather testifies for higher land plant input, but it still might evidence subsequent water column stratification due to freshwater input (by rivers). This is in agreement with high proportions of the deep-dweller *M. jansae* (Fig. 6). This interval was thus characterized by a relatively shallow, stratified water column that did not necessarily lead to permanent bottom water dysoxia/anoxia and deposition of black shales, as only few OM-rich levels occur in this interval (Fig. 7).

(5) Transgression then intensified as testified by the increasingly argillaceous content in the upper part of the section (71-89 m) (Fig. 6). The absolute abundance of nannofossils shows that the eco-space available for nannoplankton development progressively increased (Fig. 7). A trend to increased distality is also suggested by the net decrease in *Schizosphaerella* spp. abundance relative to coccolith abundance (Fig. 6). In parallel, primary production decreased, likely due to enhanced distality with respect to continental input of nutrients (Figs. 6 and 7).

5.2. Global palaeoceanographic changes around the Sinemurian/Pliensbachian boundary?

The sharp sea-level fall followed by the major transgression recorded in the Lusitanian Basin around the Sinemurian/Pliensbachian boundary seems to have been a global feature since similar sea-level variations have been evidenced in other sections of England (Hesselbo and Jenkyns, 1998), Poland (Pieńkowski, 2004), France (de Gracianski et al., 1998),

Greenland, and south Andes (Hallam, 2001). In these sections, the dramatic sea-level fall is however dated from the latest Sinemurian, followed by an important flooding across the Sinemurian/Pliensbachian transition (beginning of the Jamesoni Zone). This slight timing difference in sea-level changes could be explained by local tectonic conditions at São Pedro de Moel, as suggested by the observation of lateral facies variation in the Lusitanian Basin (see Duarte et al., 2014). However, it should be noted that the Sinemurian/Pliensbachian interval is much better defined in São Pedro de Moel section thanks to a continuous ammonite record (Comas-Rengifo et al., 2013) than in other well-studied basins. In fact, either the ammonite record is discontinuous below the boundary (for example the well-dated Yorkshire sections; see Hesselbo et al., 2000, fig. 4), the ammonite record is inferred to indicate a range interval comprised between the uppermost Sinemurian to basal Pliensbachian interval (such as in Morocco; Wilmsen et al., 2002), or a condensation or hiatus occurred across the upper Sinemurian/lower Pliensbachian (such as in France; de Graciansky et al., 1998).

In spite of the problem of exactly dating the Sinemurian/Pliensbachian boundary, on a long-term trend, these sea-level changes are however very similar, and the temporal difference is actually minor as the important flooding is recorded at the base of the Jamesoni Zone at São Pedro de Moel in a way similar to that reported by Pieńkowski (2014) for the Poland Basin. Then, sea-level changes at São Pedro de Moel do not seem to be strongly affected by local tectonic conditions and may reflect widespread sea-level variations.

This transgression at the base of the Pliensbachien could be related to tectono-eustatic sea-level changes linked to the breakup of the supercontinent Pangea, which led to the establishment of epeiric seaways such as the Hispanic Corridor that connected the Tethys and palaeo-Pacific oceans (Hallam, 1978, 1994; Smith et al., 1990, 1994; Aberhan, 2001). Several studies based on the comparison of Tethyan and eastern Pacific ammonites (Venturi et al., 2006, 2007), bivalve palaeobiogeography (Aberhan, 2001) and geochemical data (Porter et

al., 2013; Dera et al., 2015) suggest that the opening of the Hispanic Corridor was progressive, but point the latest Sinemurian-earliest Pliensbachian as the time during which it became a true seaway. This opening may have induced palaeoceanographic and palaeoclimatic changes, with more pronounced influence of warm water masses from the equatorial Tethys (e.g., van de Schootbrugge et al., 2005) and the establishment of a mega-monsoonal system above northwestern Europe with intensified summer monsoons (southeast trade winds; Röhl et al. 2001). Draining of freshwater into the Tethys, resulting from intense summer monsoons and high runoff, led to increased water column stratification (van de Schootbrugge et al., 2005) as suggested here for the interval following the forced regression at the base of Pliensbachian.

Interestingly, the opening of the Hispanic Corridor may have played a role in the first occurrence of the genus *Similiscutum* with placolith-type coccoliths, through the development of environmental conditions favourable for placolith-coccoliths that became dominant over murolith-coccoliths by the end of the early Jurassic. It has indeed already been hypothesized that the palaeoceanographic/palaeoclimatic changes subsequent to the opening of this gateway may have induced the global radiation of dinoflagellates (van de Schootbrugge et al., 2005) and of the *Lithiotis* Fauna (peculiar genera of bivalves; Franceschi et al., 2014) during the early Pliensbachian. Alternatively, placolith-coccoliths may have originated in the Pacific Realm and colonized Tethyan waters following the opening of the Hispanic Corridor.

A global ~2‰ negative shift recorded in $\delta^{13}C$ bulk carbonate, marine benthic and nektobenthic molluscs and brachiopods and terrestrial wood also marks the Sinemurian/Pliensbachian boundary in various areas (Jenkyns et al., 2002; Woodfine et al., 2008; Korte and Hesselbo, 2011). This shift suggests an increase in pCO_2, probably related to enhanced mantle-related hydrothermal activity associated with the opening of the Hispanic Corridor (Porter et al., 2013; Franceschi et al., 2014). At São Pedro de Moel, the $\delta^{13}C$ of

carbonates does not show the sudden negative shift recorded in other settings. This is unlikely due to the lack of the $\delta^{13}C$ shift record subsequent to erosion or hiatus at the base of the forced regressive system, since a negative carbon-isotope trend could be observed, with lowest values around the Sinemurian/Pliensbachian boundary and an increase in values in the earliest Pliensbachian (Figs. 4 and 6). This chemostratigraphic event seems to be correlative with $\delta^{13}C$ negative excursion recorded at Robin Hood's Bay (England; Korte and Hesselbo, 2011). According to Duarte et al. (2014), the $\delta^{13}C_{carb}$ curve across the Sinemurian/Pliensbachian of São Pedro de Moel is strongly influenced by the sedimentation of OM, which may play an important role in the control of the local seawater carbon-isotope composition.

The $\delta^{13}C_{TOC}$ does not covary with the $\delta^{13}C_{carb}$ and an opposite trend is observed between $\delta^{13}C_{TOC}$ and phytane concentration. During photosynthesis, isotopically light carbon (^{12}C) is preferentially incorporated by phytoplankton, leading to more depleted $\delta^{13}C$ values in the produced OM. The opposite trend observed between $\delta^{13}C_{TOC}$ and phytane concentration thus testifies for a major contribution of phytoplankton to OM, which supports a decrease in primary production from the Raricostatum Zone to the Jamesoni Zone. Then, it is likely that the $\delta^{13}C$ records at São Pedro de Moel are influenced by local environmental conditions and do not reflect global climatic/oceanographic changes.

6. Conclusions

Combined sedimentological, TOC, lipid biomarker and calcareous nannofossil data allow a precise characterization of the palaeoenvironmental changes occurring across the Sinemurian/Pliensbachian boundary in the Lusitanian Basin. During the Oxynotum and Raricostatum Zones (late Sinemurian), the basin was particularly restricted with a relatively low sea level. This peculiar configuration of the basin, along with climatic variations, could

account for the regular formation of black shales due to water stratification and bottom water dysoxia/anoxia. This was interrupted by storm events that allowed temporary re-oxygenation and replenishment in nutrients of surface waters thus boosting primary production. The earliest Jamesoni Zone (earliest Pliensbachian) is marked by a sharp sea-level fall followed by a major transgression. During the basal transgression, the basin was relatively shallow, with a stratified water-column that did not necessarily lead to permanent bottom water dysoxia/anoxia and deposition of black shales, and became progressively deeper and more open with the intensification of the transgression. In parallel, primary production decreased, likely due to enhanced distality with respect to continental input of nutrients.

The major transgression in the earliest Pliensbachian is probably related to tectono-eustatic sea-level changes linked to the breakup of the Pangea, which led to the opening of the Hispanic Corridor that occurred during latest Sinemurian-earliest Pliensbachian. The palaeoceanographic and palaeoclimatic changes induced by this opening may have played a role in the diversification of coccolithophores with the first occurrence or colonization of Tethyan waters by placolith-type coccoliths, which were eventually very successful and became dominant over murolith-coccolith by the end of early Jurassic. The $\delta^{13}C$ records at São Pedro de Moel are likely influenced by local environmental conditions, and do not reflect in the present case global climatic/oceanographic changes.

The present work highlights the necessity of using a multi-proxy approach to obtain a more comprehensive picture of the environmental context in which placoliths first occurred. Still, more studies in other epicontinental basins of the western Tethys would be needed to better constrain these palaeoceanographic/palaeoclimatic changes and to understand how they may have induced phytoplankton radiation. Also, in future works, the degree of restriction in anoxic marine basins, such as the Lusitanian Basin, should be quantified, using for example trace-metal concentration data.

Acknowledgments

We would like to thank Thomas Algeo, Darren Gröcke and an anonymous reviewer for their constructive comments that helped to significantly improve the quality of the manuscript. We thank François Martineau and François Fourel (Université Lyon 1, France) for their help and expertise in isotopic analyses. LVD had the support of Fundação para a Ciência e Tecnologia (FCT), through the strategic project UID/MAR/04292/2013 granted to MARE. EM and BP were funded by the PAUILF and Syster-Intervie (INSU) projects. Slides used for calcareous nannofossil study are curated at the Collections de Géologie de Lyon, Université Lyon 1 (reference number: FSL 765001 to FSL 765110).

References

Aberhan, M., 2001. Bivalve palaeobiogeography and the Hispanic Corridor: time of opening and effectiveness of a proto-Atlantic seaway. Palaeogeogr. Palaeoclimatol. Palaeoecol. 165, 375–394.

Antunes, M.T., Rocha, R.B., Wenz, S., 1981. Faunule ichtyologique du Lias inférieur de São Pedro de Moel, Portugal. Ciênc. Terra 6, 101–116.

Bassoulet, J.P., Elmi, S., Poisson, A., Cecca, F., Bellion, Y., Guiraud, R., Baudin, F., 1993. MidToarcian. In: Dercourt, J., Ricou, L.E., Vrielynck, B. (Eds.), "Atlas Tethys palaeoenvironmental maps". BEICIP-FRANLAB, Rueil-Malmaison, pp. 63–84.

Beaufort, L., 1991. Adaptation of the random settling method for quantitative studies of calcareous nannofossils. Micropaleontology 37, 415–418.

568 Behar, F., Beaumont, V., De B. Penteado, H.L., 2001. Rock-Eval 6 technology: performances
569 and developments. Oil & Gas Science and Technology-Rev. IFP 56 (2), 111–134. DOI:
570 10.2516/ogst:2001013.
571 Boussaha, M., Pittet, B., Mattioli, E., Duarte, L.V., 2014. Spatial characterization of the late
572 Sinemurian (Early Jurassic) palaeoenvironments in the Lusitanian Basin. Palaeogeogr.
573 Palaeoclimatol. Palaeoecol. 409, 320–339.
574 Bown, P., Lees, J.A., Young, J.R., 2004. Calcareous nannoplankton evolution and diversity
575 through time. In: Thierstein, H.R., Young, J.R. (Eds.), "Coccolithophores-From molecular
576 processes to global impacts". Springer, Berlin, pp. 481–508.
577 Bucefalo Palliani, R., Cirilli, S., Mattioli, E., 1998. Phytoplankton response and geochemical
578 evidence of the lower Toarcian relative sea level rise in the Umbria-Marche basin (Central
579 Italy). Palaeogeogr. Palaeoclimatol. Palaeoecol. 142, 33–50.
580 Comas-Rengifo, M.J., Duarte, L.V., Goy, A., Paredes, R., Silva, R.L., 2013. El Sinemuriense
581 Superior (cronozonas Oxynotum y Raricostatum) en la región de S. Pedro de Moel
582 (Cuenca Lusitánica, Portugal). In: Duarte, L.V., Silva, R.L., Azerêdo, A.C. (Eds.), "Fácies
583 carbonatadas ricas em matéria orgânica do Jurássico da Bacia Lusitânica. Novos
584 contributos paleontológicos, sedimentológicos e geoquímicos". Commun. Geol., 100, pp.
585 15–19 (Especial 1).
586 de Graciansky, P.-C., Dardeau, G., Dommergues, J.-L., Durlet, C., Marchand, D., Dumont, T.,
587 Hesselbo, S.P., Jacquin, T., Goggin, V., Meister, C., Mouterde, R., Rey, J. and Vail, P.R.,
588 1998. Ammonite biostratigraphic correlation and Early Jurassic sequence stratigraphy in
589 France: comparison with some U.K. sections. In: de Graciansky, P.-C., Hardenbol, J.,
590 Jacquin, T., Vail, P.R. (Eds.), "Mesozoic and Cenozoic Sequence Stratigraphy of European
591 Basins". Special Publication Society for Sedimentary Geology 60, pp. 583–622.

592 Deconinck, J.-F., Hesselbo, S.P., Debuisser, N., Averbuch, O., Baudin, F., Bessa, J., 2003.
593 Environmental controls on clay mineralogy of an Early Jurassic mudrock (Blue Lias
594 Formation, southern England). Int. J. Earth Sci. 92, 255–266.
595 Dera, G., Prunier, J., Smith, P.L., Haggart, J.W., Popov, E., Guzhov, A., Rogov, M., Delsate,
596 D., Thies, D., Cuny, G., Pucéat, E., Charbonnier, G., Bayon, G., 2015. Nd isotope
597 constraints on ocean circulation, paleoclimate, and continental drainage during the Jurassic
598 breakup of Pangea. Gondwana Res. 27, 1599–1615.
599 http://dx.doi.org/10.1016/j.gr.2014.02.006.
600 Didyk, B.M., Simoneit, B.R.T., Brassell, S.C., Eglinton, G., 1978. Organic geochemical
601 indicators of palaeoenvironmental conditions of sedimentation. Nature 272, 216–222.
602 Dommergues, J.-L., El Hariri, K., 2002. Endemism as a palaeobiogeographic parameter of
603 basin history illustrated by early- and mid-Liassic peri-Tethyan ammonite faunas.
604 Palaeogeogr., Palaeoclimatol., Palaeoecol. 184, 407–418.
605 Duarte, L.V., 2007. Lithostratigraphy, sequence stratigraphy and depositional setting of the
606 Pliensbachian and Toarcian series in the Lusitanian Basin (Portugal). In: Rocha, R.B. (Ed.),
607 "The Peniche Section (Portugal), Contributions of the Definition of the Toarcian GSSP".
608 Int. Subcom. Jur. Strat., pp. 17–23.
609 Duarte, L.V., Soares, A.F., 2002. Litostratigrafia das séries margo-calcárias do Jurássico
610 Inferior da Bacia Lusitânica (Portugal). Commun. Inst. Geol. Min. 89, 135–154.
611 Duarte, L.V., Wright, V.P., Fernández-López, S., Elmi, S., Krautter, M., Azerêdo, A.C.,
612 Henriques, M.H., Rodrigues, R., Perilli, N., 2004. Early Jurassic carbonate evolution in the
613 Lusitanian Basin: Facies, sequence stratigraphy and cyclicity. In: Duarte, L.V., Henriques,
614 M.H. (Eds.), "Carboniferous and Jurassic Carbonate Platforms of Iberia. 23rd IAS Meeting
615 of sedimentology, Coimbra 2004". Field Trip Guide Book I, pp. 45–71.

616 Duarte, L.V., Silva, R.L., Oliveira, L.C.V., Comas-Rengifo, M.J., Silva, F., 2010. Organic-
617 rich facies in the Sinemurian and Pliensbachian of the Lusitanian Basin, Portugal: Total
618 organic carbon and relation to transgressive–regressive facies cycles. Geol. Acta 8, 325–
619 340.
620 Duarte, L.V., Silva, R.L., Mendonça Filho, J.G., Poças Ribeiro, N., Chagas, R.B.A., 2012.
621 High resolution stratigraphy, palynofacies and source rock potential of the Água de
622 Madeiros formation (Lower Jurassic), Lusitanian Basin, Portugal. J. Pet. Geol. 35 (2), 105–
623 126.
624 Duarte, L.V., Comas-Rengifo, M.J., Silva, R.L., Paredes, R., Goy, A., 2014. Carbon isotope
625 stratigraphy and ammonite biochronostratigraphy across the Sinemurian-Pliensbachian
626 boundary in the western Iberian margin. Bull. Geosci. 89 (4), 719–736.
627 Espitalié, J., 1993. Rock Eval pyrolysis. In: Bordenave, M.L. (Ed.), "Applied Petroleum
628 Geochemistry". Technip, Paris, pp. 237–261.
629 Espitalié, J., Deroo, G., Marquis, F., 1986. La pyrolyse Rock-Eval et ses applications.
630 Troisième partie. Rev. Inst. Fr. Pét. 41 (1), 73–89.
631 Franceschi, M., Dal Corso, J., Posenato, R., Roghi, G., Masetti, D., Jenkyns, H.C., 2014.
632 Early Pliensbachian (Early Jurassic) C-isotope perturbation and the diffusion of the
633 Lithiotis Fauna: Insights from the western Tethys. Palaeogeogr. Palaeoclimatol.
634 Palaeoecol. 410, 255–263. http://dx.doi.org/10.1016/j.palaeo.2014.05.025.
635 Geisen, M., Bollmann, J., Herrle, J.O.,Mutterlose, J., Young, J.R., 1999. Calibration of the
636 random settling technique for calculation of absolute abundances of calcareous
637 nannoplankton. Micropaleontology 45, 437–442.
638 Hallam, A., 1978. Tectonism and eustasy in the Jurassic. Earth Sci. Rev. 5 (1969), 45–68.
639 Hallam, A., 1994. An outline of phanerozoic biogeography. Oxford Biogeogr. Ser. 10, 1–246.

640 Hallam, A., 2001. A review of the broad pattern of Jurassic sea level changes and their
641 possible causes in the light of current knowledge. Palaeogeogr. Palaeoclimatol. Palaeoecol.
642 167, 23–37.
643 Hesselbo, S.P., Jenkyns, H.C., 1998. British Lower Jurassic sequence stratigraphy. In: de
644 Graciansky, P.-C., Hardenbol, J., Jacquin, T., Vail, P.R. (Eds.), "Mesozoic and Cenozoic
645 Sequence Stratigraphy of European Basins". Special Publication Society for Sedimentary
646 Geology 60, pp. 561–581.
647 Hesselbo, S.P., Meister, C., Gröcke, D.R., 2000. A potential global stratotype for the
648 Sinemurian-Pliensbachian boundary (Lower Jurassic), Robin Hood's Bay, UK: ammonite
649 faunas and isotope stratigraphy. Geol. Mag. 137 (6), 601–607. DOI:
650 10.1017/S0016756800004672.
651 Jenkyns, H.C., Jones, C.E., Gröcke, D.R., Hesselbo, S.P., Parkinson, D.N., 2002.
652 Chemostratigraphy of the Jurassic System: applications, limitations and implications for
653 palaeoceanography. J. Geol. Soc. London 159, 351–378. DOI: 10.1144/0016-764901-130.
654 Knoll, A.H., Summons, R.E., Waldbauer, J.R., Zumberge, J.E., 2007. The geological
655 succession of primary producers in the oceans. In: Falkowski, P., Knoll, A.H. (Eds.), "The
656 Evolution of Primary Producers in the Sea". Academic Press, Boston, pp. 133–163.
657 Kodner, R.B., Summons, R.E., Pearson, A., King, N., Knoll, A.H., 2008. Sterols in a
658 unicellular relative of the metazoans. Proc. Natl. Acad. Sci. 105 (29), 9897–9902.
659 Korte, C., Hesselbo, S.P., 2011. Shallow marine carbon and oxygen isotope and elemental
660 records indicate icehouse–greenhouse cycles during the Early Jurassic. Paleoceanography
661 26, PA4219. http://dx.doi.org/10.1029/2011PA002160.
662 Manspeizer, W., 1988. Triassic-Jurassic rifting and opening of the Atlantic: an overview. In:
663 Manspeizer, W. (Ed.), "Triassic-Jurassic rifting, Continental breakup and the origin of the
664 Atlantic Ocean and passive margins". Dev. Geotect. 22, pp. 41–72.

Mattioli, E., 1997. Nannoplankton productivity and diagenesis in the rhythmically bedded Toarcian–Aalenian Fiuminata section (Umbria–Marche Apennine, central Italy). Palaeogeogr. Palaeoclimatol. Palaeoecol. 130, 113–133.

Mattioli, E., Pittet, B., 2002. Contribution of calcareous nannoplankton to carbonate deposition: a new approach applied to the Early Jurassic of central Italy. Mar. Micropaleontol. 45, 175–190.

Mattioli, E., Pittet, B., 2004. Spatial and temporal distribution of calcareous nannofossils along a proximal–distal transect in the Lower Jurassic of the Umbria–Marche Basin (central Italy). Palaeogeogr. Palaeoclimatol. Palaeoecol. 205, 295–316.

Mattioli, E., Pittet, B., Suan, G., Mailliot, S., 2008. Calcareous nannoplankton across Early Toarcian anoxic event: Implications for paleoceanography within the western Tethys. Paleoceanography 23, PA3208. http://dx.doi.org/10.1029/2007PA001435.

Mattioli, E., Plancq, J., Boussaha, M., Duarte, L.V., Pittet, B., 2013. Calcareous nannofossil biostratigraphy: New data from the Lower Jurassic of the Lusitanian Basin. Commun. Geol. 100, 69–76 (Especial I).

Meister, C., Aberhan, M., Blau, J., Dommergues, J.-L., Feist-Burkhardt, S., Hailwood, E.A., Hart, M., Hesselbo, S.P., Hounslow, M.W., Hylton, M., Morton, N., Page, K., Price, G.D., 2006. The Global Boundary Stratotype Section and Point (GSSP) for the base of the Pliensbachian Stage (Lower Jurassic), Wine Haven, Yorkshire, UK. Episodes 29 (2), 93–106.

Meister, C., Dommergues, J.-L., Rocha, R.B., 2012. Ammonites from the *Apoderoceras* beds (Early Pliensbachian) in São Pedro de Muel (Lusitanian Basin, Portugal). Bull. Geosci. 87(3), 407–430. DOI: 10.3140/bull.geosci.1325.

Mouterde, R., 1967. Le Lias du Portugal. Vue d'ensemble et division en zones. Comun. Serv. Geol. Portugal 52, 209–226.

690 Mudie, P.J., Marret, F., Rochon, A., Aksu, A.E., 2010. Non-pollen palynomorphs in the Black
691 Sea corridor. Veget. Hist. Archaeobot. 19, 531–544. DOI: 10.1007/s00334-010-0268-9.
692 Noël, D., Busson, G., Cornée, A., Mangin, A.M., 1994. Le nannoplancton calcaire et la
693 formation des alternances calcaires-marnes dans le Lias des bassins de Marches-Ombrie
694 (Italie). Riv. ltal. Paleont. Strat. 99, 515–550.
695 Ourisson, G., Rohmer, M., Poralla, K., 1987. Prokaryotic hopanoids and other polyterpenoid
696 sterol surrogates. Annu. Rev. Microbiol. 41, 301–333.
697 Peters, K.E., Walters, C.C., Moldowan, J.M., 2005. The Biomarker Guide, 2nd ed. Cambridge
698 University Press, Cambridge.
699 Pieńkowski, G., 2004. The epicontinental Lower Jurassic of Poland. Polish Geol. Inst. Sp.
700 Pap. 12, 1–154.
701 Pieńkowski, G., 2014. The first Early Jurassic ammonite find in central Poland. Volumina
702 Jurassica XII (1), 99–104.
703 Pittet, B., Mattioli, E., 2002. The carbonate signal and calcareous nannofossil distribution in
704 an Upper Jurassic section (Balingen–Tieringen, Late Oxfordian, southern Germany).
705 Palaeogeogr. Palaeoclimatol. Palaeoecol. 179, 71– 96.
706 Poças Ribeiro, N., Mendonça Filho, J.G., Duarte, L.V., Silva, R.L., Mendonça, J.O., Silva,
707 T.F., 2013. Palynofacies and organic geochemistry of the Sinemurian carbonate deposits in
708 the western Lusitanian Basin (Portugal): Coimbra and Água de Madeiros formations. Int. J.
709 Coal Geol. 111, 37–52. DOI: 10.1016/j.coal.2012.12.006.
710 Porter, S.J., Selby, D., Suzuki, H., Gröcke, D., 2013. Opening of a trans Pangaean marine
711 corridor during the Early Jurassic: insights from osmium isotopes across the Sinemurian–
712 Pliensbachian GSSP, Robin Hood's Bay, UK. Palaeogeogr. Palaeoclimatol. Palaeoecol.
713 375, 50–58.

Reggiani, L., Mattioli, E., Pittet, B., Duarte, L.V., Oliveira, L.C.V., Comas-Rengifo, M.J., 2010. Pliensbachian (Early Jurassic) calcareous nannofossils from the Peniche section (Lusitanian Basin, Portugal): a clue for palaeoenvironmental reconstructions. Mar. Micropal. 75, 1–16. DOI: 10.1016/j.marmicro.2010.02.002.

Röhl, H.J., Schmid Röhl, A.,Wolfgang, O., Frimmel, A., Lorenz, S., 2001. The Posidonia Shale (Lower Toarcian) of SW Germany: An oxygen depleted ecosystem controlled by sea level and palaeoclimate. Palaeogeogr. Palaeoclimatol. Palaeoecol. 165, 27–52.

Rohmer, M., Bouvier-Nave, P., Ourisson, G., 1984. Distribution of hopanoid triterpenes in prokaryotes. J. Gen. Microbiol. 130, 1137–1150.

Rosales, I., Quesada, S., Robles, S., 2004. Palaeotemperature variations of Early Jurassic seawater recorded in geochemical trends of belemnites from the Basque Cantabrian basin, northern Spain. Palaeogeogr. Palaeoclimatol. Palaeoecol. 203, 253–275.

Roth, P.H., 1984. Preservation of calcareous nannofossils and fine grained carbonate particles in mid cretaceous sediments from the southern Angola Basin. In: Hay, W.W., Sibuet, J.C., et al. (Eds.), Init. Rept. DSDP "Initial reports of the Deep Sea Drilling Project, Volume 75". Washington, D.C., U.S. Government Printing Office, pp. 651–655.

Scotese, C.R., 2001. Atlas of Earth History, Volume 1, Paleogeography. PALEOMAP Project, Arlington, Texas, 52 pp.

Silva, R.L, Duarte, L.V., Mendonça Filho, J.G., 2013. Optical and geochemical characterization of Upper Sinemurian (Lower Jurassic) fossil wood from the Lusitanian Basin (Portugal). Geochem. J. 47(5), 489–498. DOI: 10.2343/geochemj.2.0270.

Smith, A.G., Smith, D.G., Funnel, B.M., 1994. Atlas of Mesozoic and Cenozoic Coastlines. Cambridge University Press, 99 pp.

Smith, P.L., Westermann, G.E.G., Stanley, G.D., Yancey, T.E., 1990. Paleobiogeography of the ancient Pacific. Science 249, 680–681.

739 Soares, A.F., Rocha, R.B., Elmi, S., Henriques, M.H., Mouterde, R., Almeras, Y., Ruget, C.,
740 Marques, J., Duarte, L.V., Carapito, C., Kullberg, J.C., 1993. Le sous bassin nord
741 lusitanien (Portugal) du Trias au Jurassique moyen: Histoire d'un "rift avorté". C. R. Acad.
742 Sci. Paris 317, 1659–1666.
743 Tremolada, F., van de Schootbrugge, B., Erba, E., 2005. Early Jurassic schizosphaerellid
744 crisis in Cantabria, Spain: Implications for calcification rates and phytoplankton evolution
745 across the Toarcian oceanic anoxic event. Paleoceanography 20, 1–11.
746 van de Schootbrugge, B., Bailey, T.R., Rosenthal, Y., Katz, M.E., Wright, J.D., Miller, K.G.,
747 Feist Burkhardt, S., Falkowski, P.G., 2005. Early Jurassic climate change and the radiation
748 of organic walled phytoplankton in the Tethys Ocean. Paleobiology 31, 73–97.
749 Vanney, J.R., Mougenot, D., 1981. La plateforme continentale du Portugal et les provinces
750 adjacentes: Analyse géomorphologique. Mém. Serv. Géol. Portugal 28, 81.
751 Venturi, F., Billotta, M., Ricci, C., 2006. Comparison between western Tethys and eastern
752 Pacific ammonites: further evidence for a possible late Sinemurian–early Pliensbachian
753 trans-Pangaean marine connection. Geol. Mag. 143 (5), 699–711.
754 Venturi, F., Nannarone, C., Billotta, M., 2007. Ammonites from the early Pliensbachian of the
755 Furlo Pass (Marche, Italy): biostratigraphic and paleobiogeographic implications. Boll.
756 Soc. Paleontol. Ital. 46 (1), 1–31.
757 Volkman, J.K., Barrett, S.M., Blackburn, S.I., Mansour, M.P., Sikes, E.L., Gelin, F., 1998.
758 Microalgal biomarkers: A review of recent research developments. Org. Geochem. 29 (5-
759 7), 1163–1179.
760 Volkman, J.K., Barrett, S.M., Blackburn, S.I., 1999. Eustigmatophyte microalgae are potential
761 sources of C_{29} sterols, C_{22}–C_{28} n-alcohols and C_{28}–C_{32} n-alkyl diols in freshwater
762 environments. Org. Geochem. 30, 307–318.

763 Wilmsen, M., Blau, J., Meister, C., Mehdi, M., Neuweiler, F., 2002. Early Jurassic
764 (Sinemurian to Toarcian) ammonites from the central High Atlas (Morocco) between Er-
765 Rachidia and Rich. Revue Paléobiol. Genève 21, 149-175 ISSN 0253-6730.
766 Woodfine, R.G., Jenkyns, H.C., Sarti, M., Baroncini, F., Violante, C., 2008. The response of
767 two Tethyan carbonate platforms to the early Toarcian (Jurassic) oceanic anoxic event:
768 environmental change and differential subsidence. Sedimentology 55, 1011–1028.
769 Young, J.R., 1994. Functions of coccoliths. In: Winter, A., Siesser, W. (Eds.),
770 "Coccolithophores". Cambridge Univ. Press, Cambridge, pp. 63– 82.
771

772 **Figure captions**

773

774 **Figure 1. A)** Location of the São Pedro de Moel section (adapted from Reggiani et al., 2010).
775 **B)** Palaeogeographic map of the early Jurassic (after Scotese, 2001) and location of the São
776 Pedro de Moel section (Lusitanian Basin) during the early Jurassic (modified after Bassoulet
777 et al., 1993). **C)** Distribution of the studied section on a schematic proximal–distal profile
778 through the Lusitanian Basin during the early Jurassic; BF means Berlenga-Farilhões
779 (modified after Vanney and Mougenot, 1981).

780

781 **Figure 2.** Stratigraphic log of the São Pedro de Moel composite section. Biostratigraphic data
782 (Ammonite and Calcareous nannofossil Zones; calcareous nannofossil events) are from
783 Comas-Rengifo et al. (2013) and Mattioli et al. (2013). Depositional environment and
784 sequence stratigraphy are from Boussaha et al. (2014).

785

786 **Figure 3.** Absolute (nannofossils/g of sediment) and relative (%) species-specific nannofossil
787 abundances during the Sinemurian/Pliensbachian of São Pedro de Moel. The relative

abundances of the nannoliths *Schizosphaerella* spp. and *Orthogonoides* spp. were calculated over the total nannofossil content, while species-specific relative abundances of various coccolith species were calculated over the total coccolith content. The grey band represents the HCS-bearing tempestite interval, where no samples were collected.

Figure 4. Bulk geochemistry and lipid-biomarker data during the Sinemurian/Pliensbachian of São Pedro de Moel. **A)** Total organic carbon (TOC) content (wt.%). Data from Duarte et al. (2012) are reported in grey. **B)** Phytane content (µg/gTOC), indicative of phytoplanktonic productivity. **C)** Sterane content (µg/gTOC), indicating the contribution of algae and metazoan (C_{27} steranes), of chlorophyll-c algae (C_{28} steranes), and of higher land plants (C_{29} steranes). **D)** Hopane content (µg/gTOC). **E)** Steranes/(Steranes + Hopanes) ratio, indicative of relative changes among eukaryotic and bacterial sources. **F)** Carbon isotope composition of carbonates ($\delta^{13}C_{carb}$; ‰). Data from Duarte et al. (2014) are reported in grey. **F)** Carbon isotope composition of organic matter ($\delta^{13}C_{TOC}$; ‰). Note that the horizontal scale for Steranes is different from the one for Phytane and Hopanes.

Figure 5. Rock-Eval pyrolysis data. **A)** The plot of HI (mgHC/gTOC) *vs*. Tmax (°C) indicates that organic matter is immature and has undergone only minor diagenesis. **B)** The plot of HI (mgHC/gTOC) *vs*. OI ($mgCO_2$/gTOC) shows that organic matter is of Type II, dominantly of marine origin. The boundary lines that denote the different kerogen types are from Espitalié et al. (1986). The different symbols indicate the samples that are in the "outer-ramp-offshore", "mid to outer-ramp" and the "mid to inner-ramp" environments. This shows that there is no distinct grouping of organic matter type versus palaeoenvironment.

Figure 6. Synthesis of the main data that allow distinguishing five intervals, noted (1) to (5), of varying sea level and primary productivity during the Sinemurian/Pliensbachian of São Pedro de Moel. TOC and $\delta^{13}C_{carb}$ data from Duarte et al. (2012, 2014) are represented by 3-points moving average curves. The first occurrence of placolith-type coccoliths and the presumed timing of the opening of the Hispanic Corridor are also reported.

Figure 7. Schematic representations of the palaeoceanographic evolution at São Pedro de Moel during the Sinemurian/Pliensbachian (modified after Boussaha et al., 2014). The five intervals, noted (1) to (5), are those of varying sea level and primary productivity presented in Figure 6 and described in the text.

Figure 1

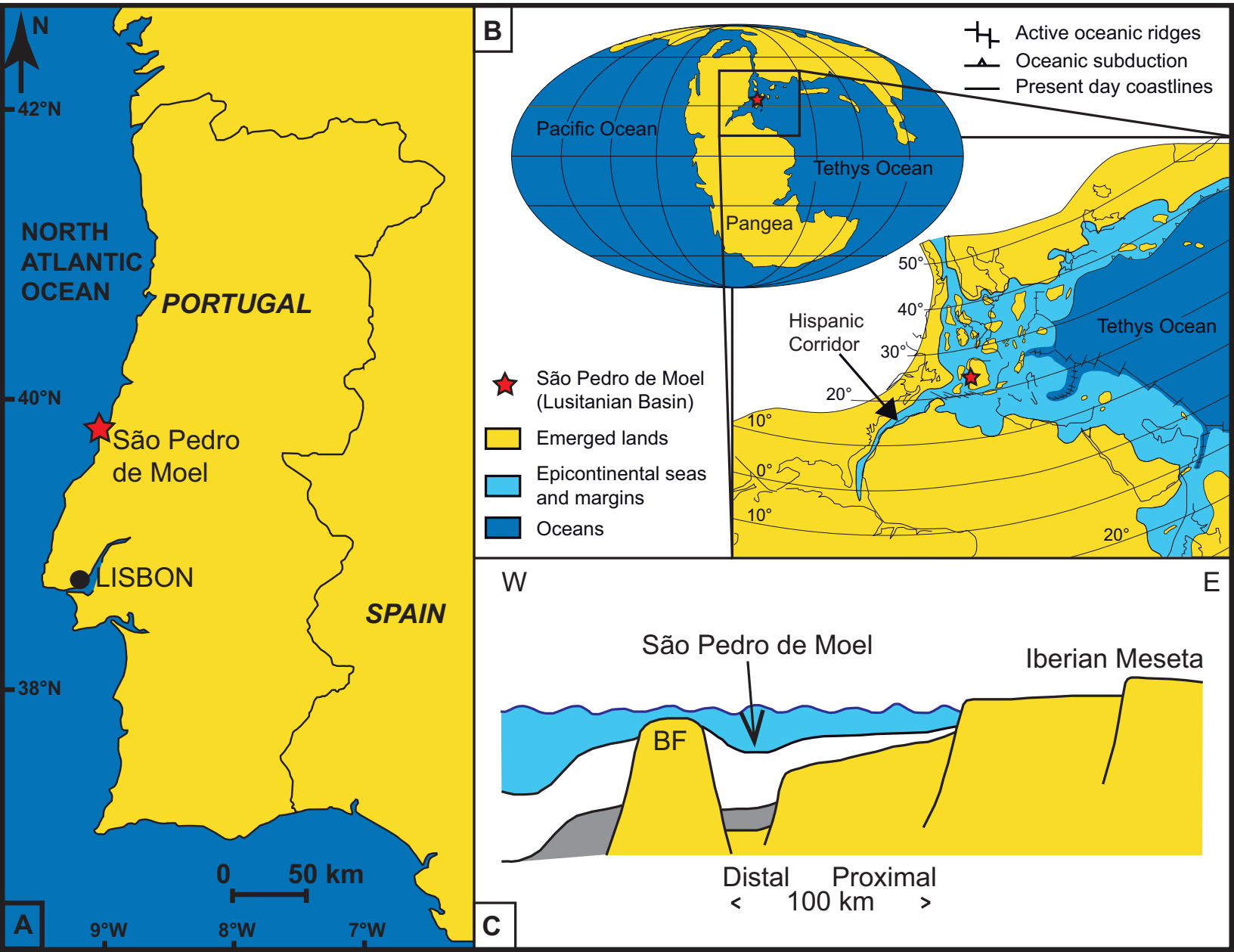
A
N
42°N
40°N
38°N
NORTH ATLANTIC OCEAN
PORTUGAL
SPAIN
São Pedro de Moel
LISBON
0
50 km
9°W
8°W
7°W
B
Active oceanic ridges
Oceanic subduction
Present day coastlines
Pacific Ocean
Tethys Ocean
Pangea
Hispanic Corridor
Tethys Ocean
50°
40°
30°
20°
10°
0°
10°
20°
São Pedro de Moel (Lusitanian Basin)
Emerged lands
Epicontinental seas and margins
Oceans
C
W
E
São Pedro de Moel
Iberian Meseta
BF
Distal
Proximal
< 100 km >

Figure 2

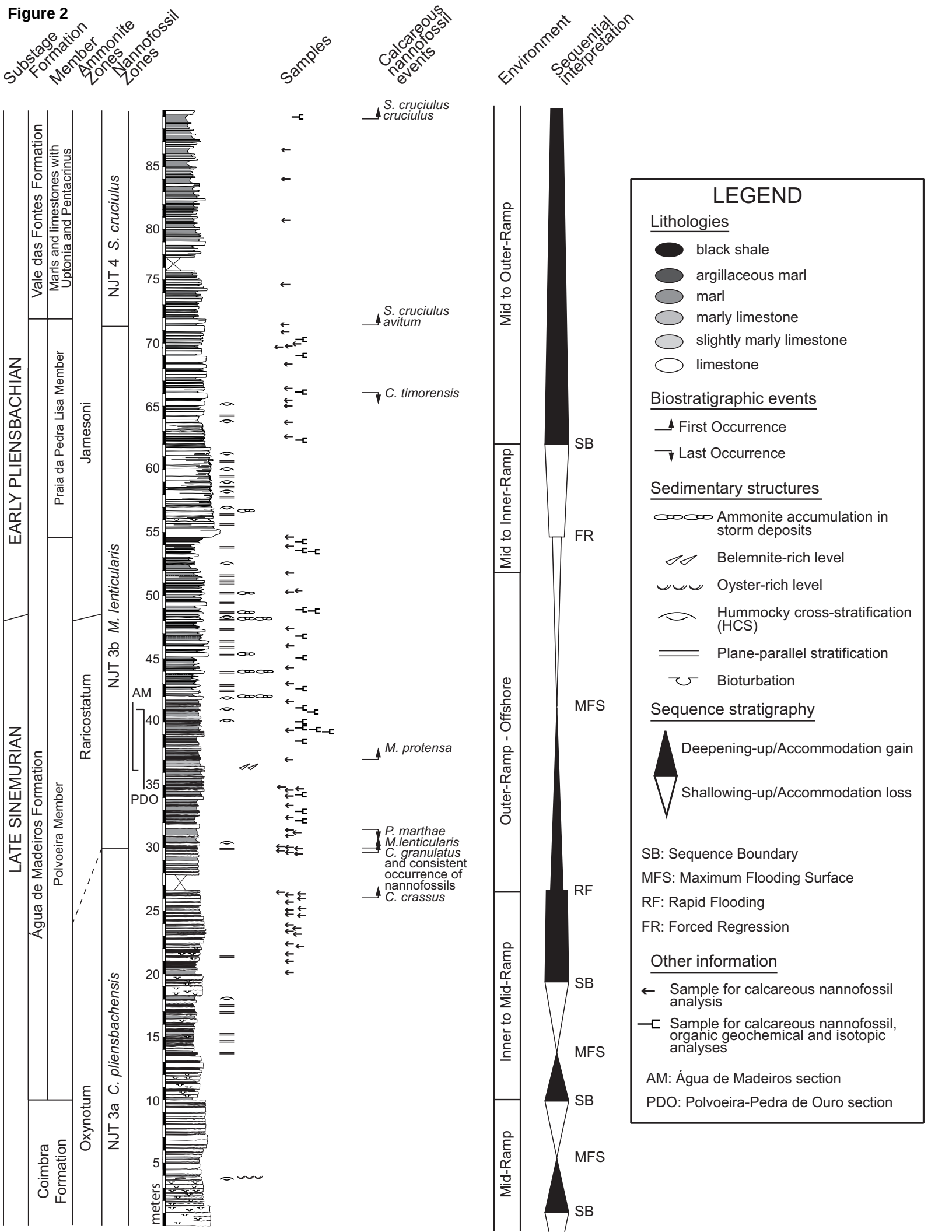
Substage
Formation
Member
Ammonite Zones
Nannofossil Zones
Samples
Calcareous nannofossil events
Environment
Sequential interpretation
LATE SINEMURIAN
EARLY PLIENSBACHIAN
Coimbra Formation
Água de Madeiros Formation
Vale das Fontes Formation
Polvoeira Member
Praia da Pedra Lisa Member
Marls and limestones with Uptonia and Pentacrinus
Oxynotum
Raricostatum
Jamesoni
NJT 3a C. pliensbachensis
NJT 3b M. lenticularis
NJT 4 S. cruciulus
AM
PDO
meters
S. cruciulus cruciulus
S. cruciulus avitum
C. timorensis
M. protensa
P. marthae
M.lenticularis
C. granulatus
and consistent occurrence of nannofossils
C. crassus
Mid-Ramp
Inner to Mid-Ramp
Outer-Ramp - Offshore
Mid to Inner-Ramp
Mid to Outer-Ramp
SB
FR
MFS
RF
SB
MFS
SB
MFS
SB
LEGEND
Lithologies
black shale
argillaceous marl
marl
marly limestone
slightly marly limestone
limestone
Biostratigraphic events
First Occurrence
Last Occurrence
Sedimentary structures
Ammonite accumulation in storm deposits
Belemnite-rich level
Oyster-rich level
Hummocky cross-stratification (HCS)
Plane-parallel stratification
Bioturbation
Sequence stratigraphy
Deepening-up/Accommodation gain
Shallowing-up/Accommodation loss
SB: Sequence Boundary
MFS: Maximum Flooding Surface
RF: Rapid Flooding
FR: Forced Regression
Other information
Sample for calcareous nannofossil analysis
Sample for calcareous nannofossil, organic geochemical and isotopic analyses
AM: Água de Madeiros section
PDO: Polvoeira-Pedra de Ouro section

Figure 3

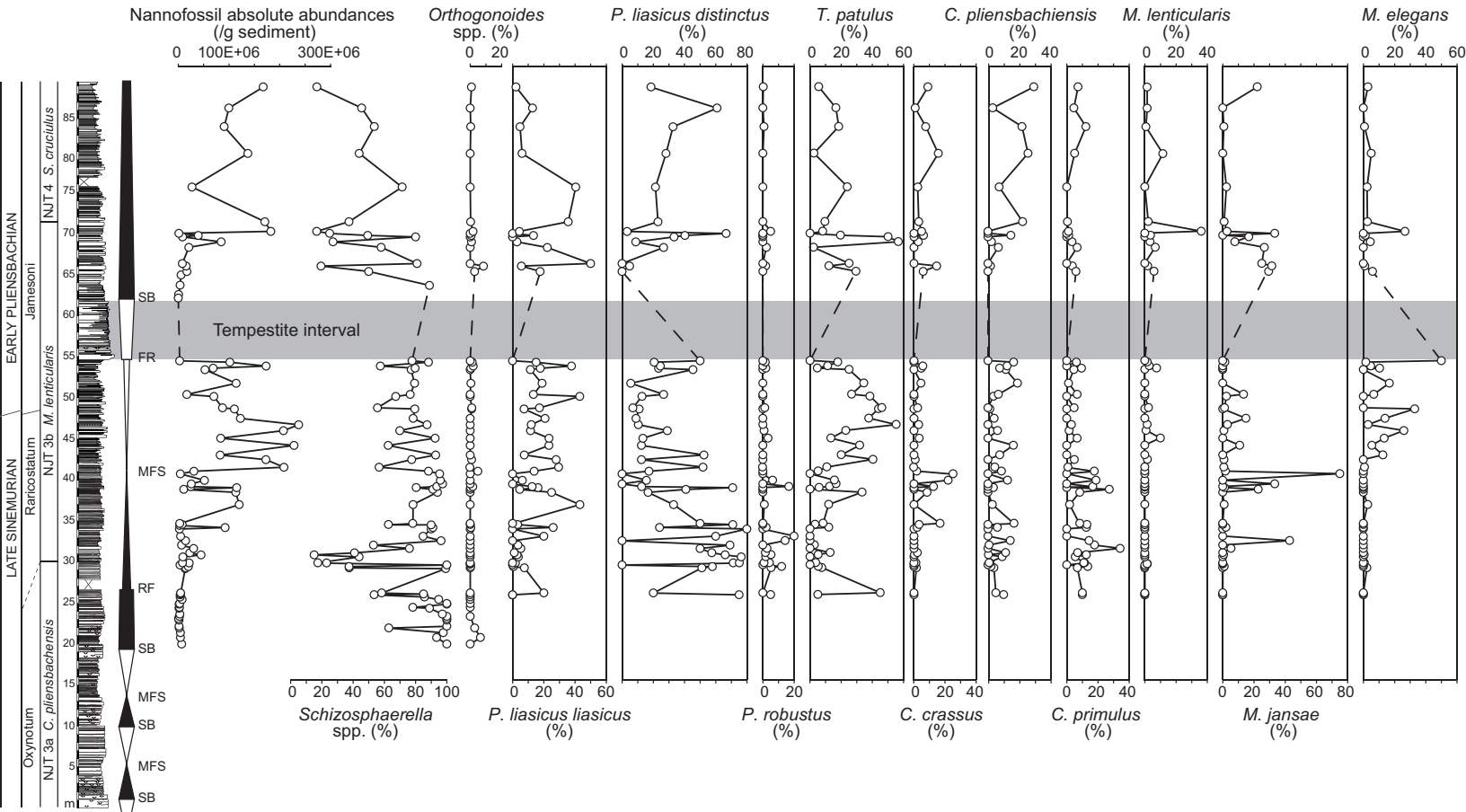
Nannofossil absolute abundances (/g sediment)
0 100E+06 300E+06
Orthogonoides spp. (%)
0 20
P. liasicus distinctus (%)
0 20 40 60 80
T. patulus (%)
0 20 40 60
C. pliensbachiensis (%)
0 20 40
M. lenticularis (%)
0 20 40
M. elegans (%)
0 20 40 60
EARLY PLIENSBACHIAN
LATE SINEMURIAN
Jamesoni
Raricostatum
Oxynotum
NJT 4
NJT 3b
NJT 3a
S. cruciulus
M. lenticularis
C. pliensbachensis
Tempestite interval
SB
FR
MFS
RF
SB
MFS
SB
MFS
SB
m
Schizosphaerella spp. (%)
0 20 40 60 80 100
P. liasicus liasicus (%)
0 20 40 60
P. robustus (%)
0 20
C. crassus (%)
0 20 40
C. primulus (%)
0 20 40
M. jansae (%)
0 20 40 60 80

Figure 4

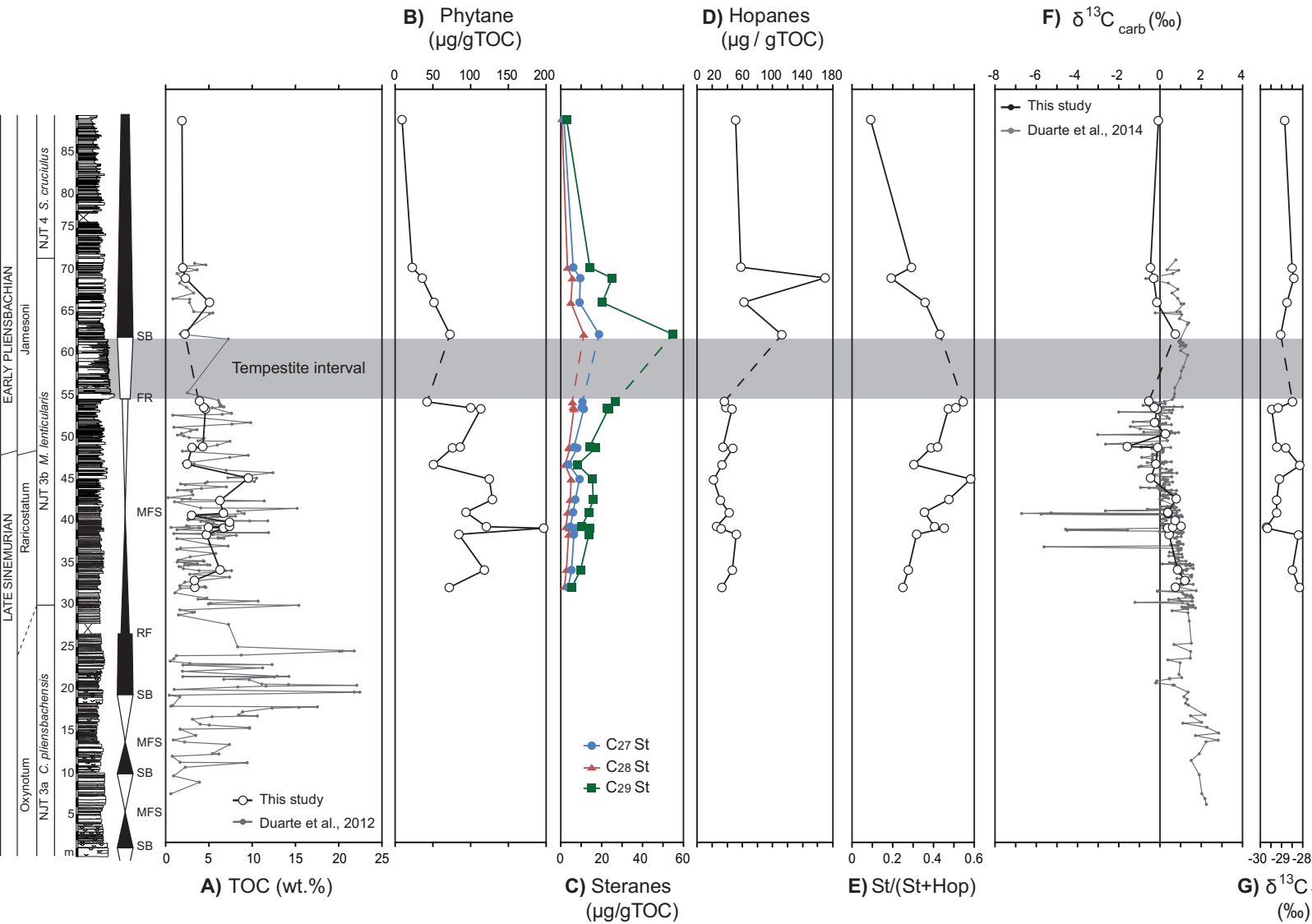
B) Phytane (µg/gTOC)
D) Hopanes (µg / gTOC)
F) δ13C carb (‰)
EARLY PLIENSBACHIAN
LATE SINEMURIAN
Jamesoni
Raricostatum
Oxynotum
NJT 4 S. cruciulus
NJT 3b M. lenticularis
NJT 3a C. pliensbachensis
SB
FR
MFS
RF
SB
MFS
SB
MFS
SB
Tempestite interval
This study
Duarte et al., 2012
C27 St
C28 St
C29 St
This study
Duarte et al., 2014
A) TOC (wt.%)
C) Steranes (µg/gTOC)
E) St/(St+Hop)
G) δ13C TOC (‰)

Figure 5

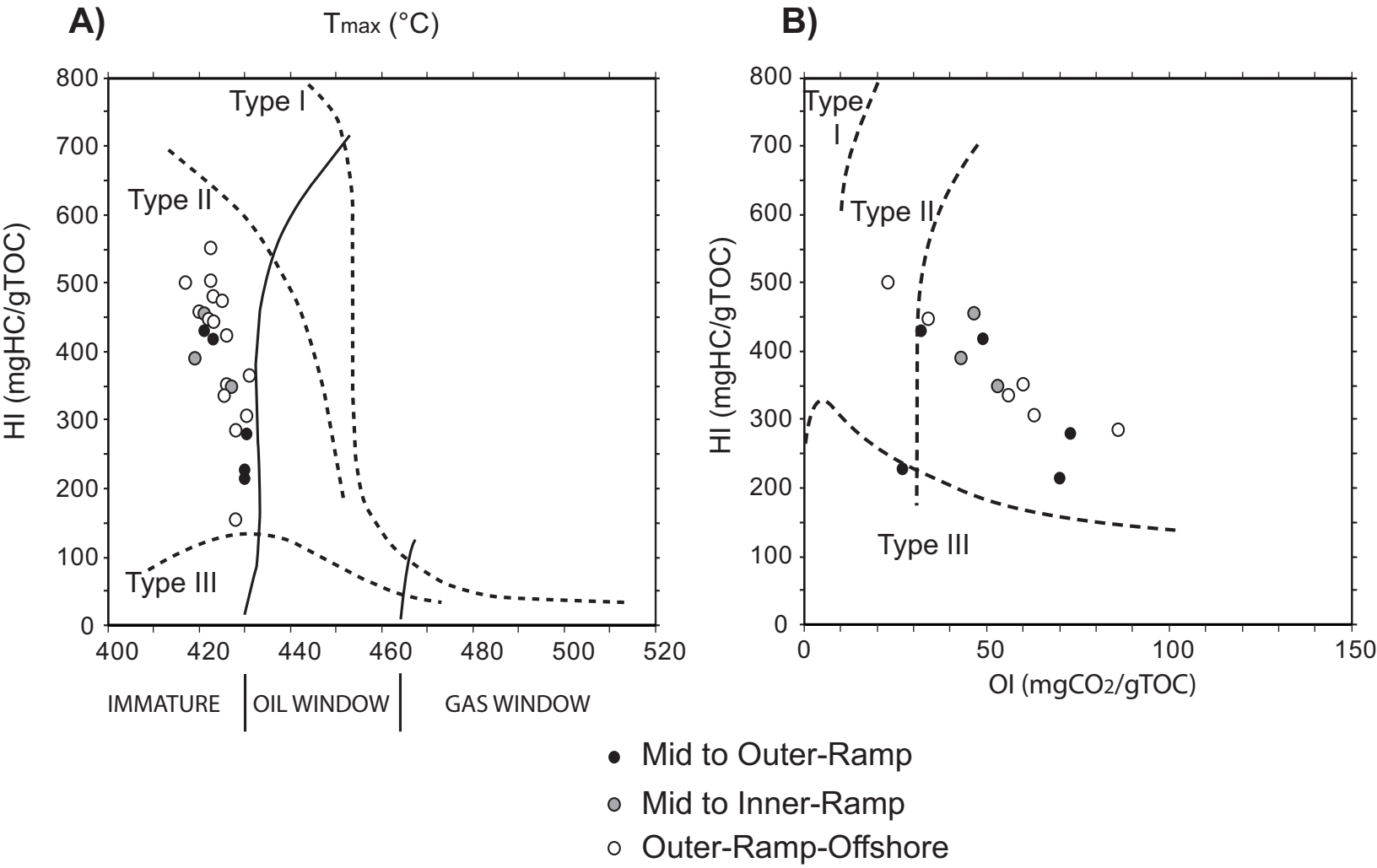
A)
Tmax (°C)
HI (mgHC/gTOC)
Type I
Type II
Type III
IMMATURE
OIL WINDOW
GAS WINDOW
B)
OI (mgCO2/gTOC)
Mid to Outer-Ramp
Mid to Inner-Ramp
Outer-Ramp-Offshore

Figure 6

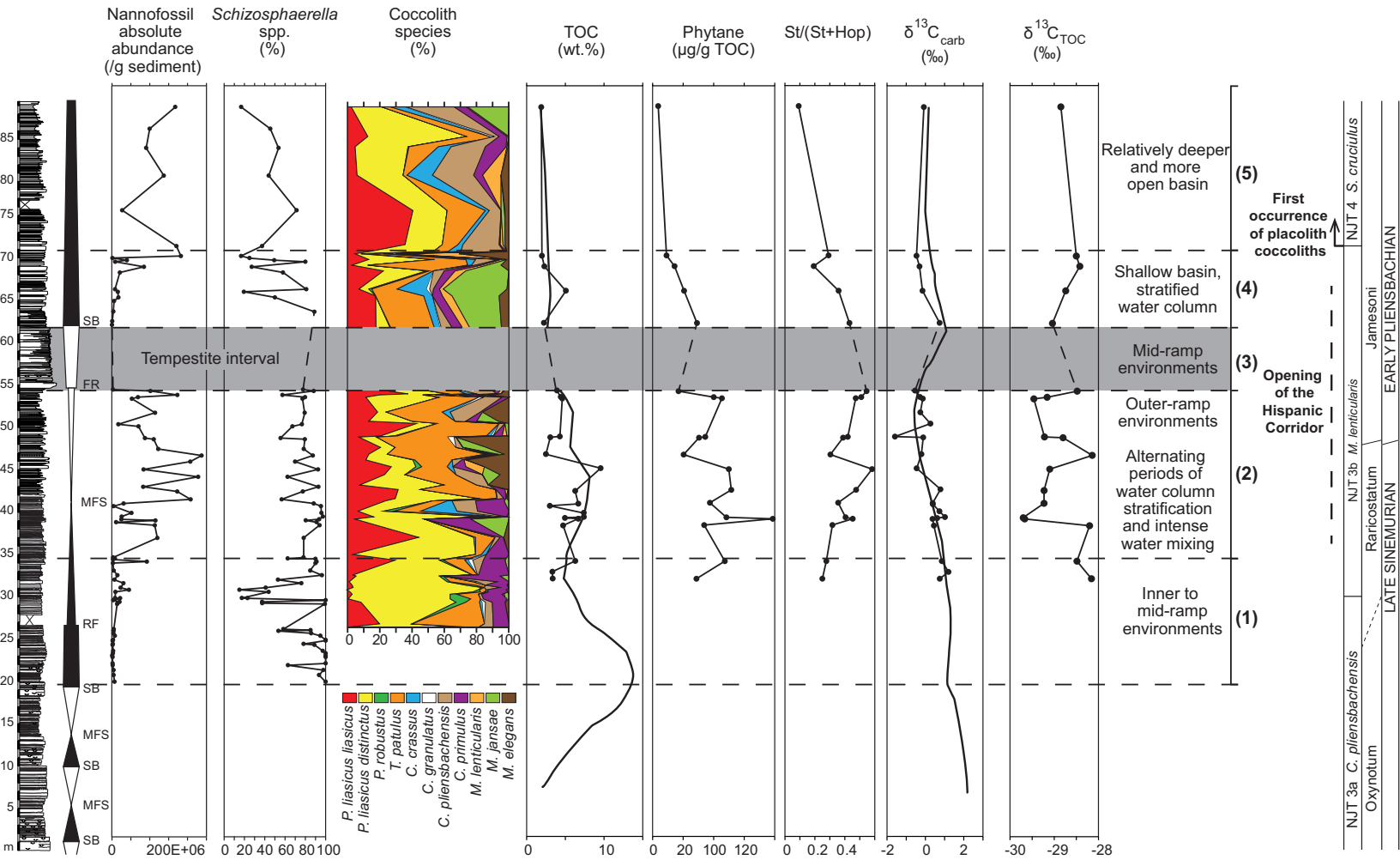
Nannofossil absolute abundance (/g sediment)
Schizosphaerella spp. (%)
Coccolith species (%)
TOC (wt.%)
Phytane (µg/g TOC)
St/(St+Hop)
δ13Ccarb (‰)
δ13CTOC (‰)
m
SB
FR
MFS
RF
SB
MFS
SB
MFS
SB
Tempestite interval
0 200E+06
0 20 40 60 80 100
0 20 40 60 80 100
0 10
0 20 100 120
0 0.2 0.4
-2 0 2
-30 -29 -28
P. liasicus liasicus
P. liasicus distinctus
P. robustus
T. patulus
C. crassus
C. granulatus
C. pliensbachensis
C. primulus
M. lenticularis
M. jansae
M. elegans
Relatively deeper and more open basin
(5)
Shallow basin, stratified water column
(4)
Mid-ramp environments
(3)
Outer-ramp environments
Alternating periods of water column stratification and intense water mixing
(2)
Inner to mid-ramp environments
(1)
First occurrence of placolith coccoliths
Opening of the Hispanic Corridor
NJT 4 S. cruciulus
NJT 3b M. lenticularis
NJT 3a C. pliensbachensis
Jamesoni
Raricostatum
Oxynotum
EARLY PLIENSBACHIAN
LATE SINEMURIAN

Figure 7

(5) Intensification of trangression, deeper and more open basin, low primary productivity

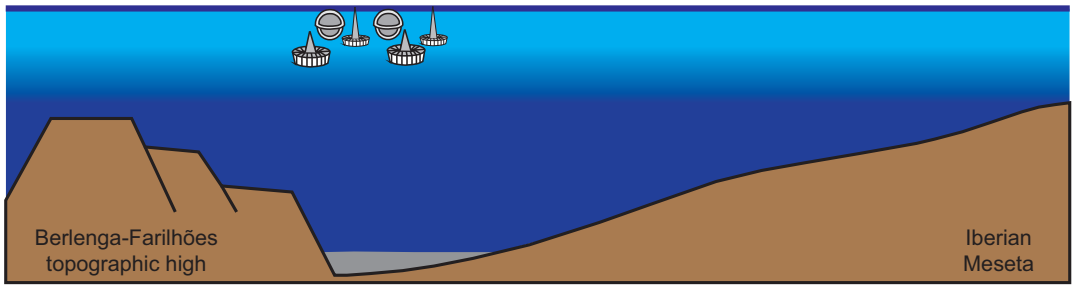

(4) Transgression, stratified water column, decrease in primary productivity

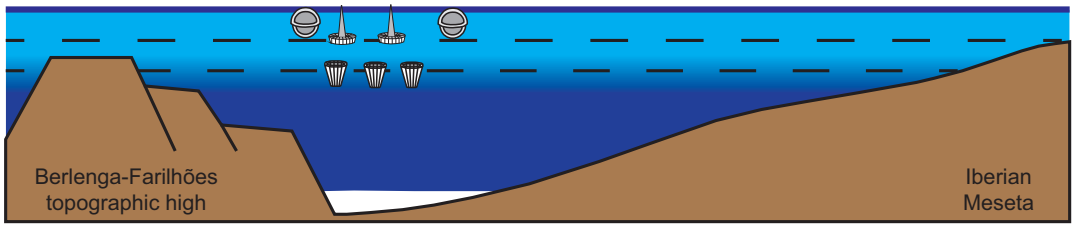

(3) Sharp sea-level fall, well oxygenated basin waters

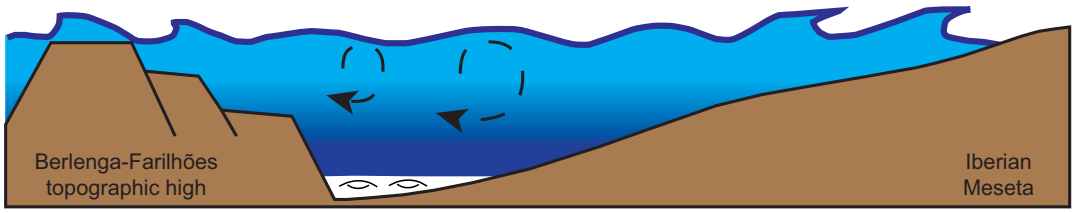

(2) Rapid flooding, expansion of the photic zone, high primary productivity
Alternation between:

- Periods of intense water mixing

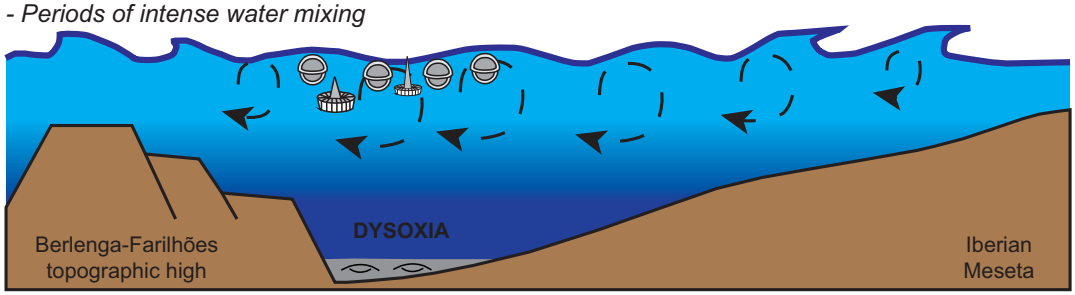

- Periods of water column stratification

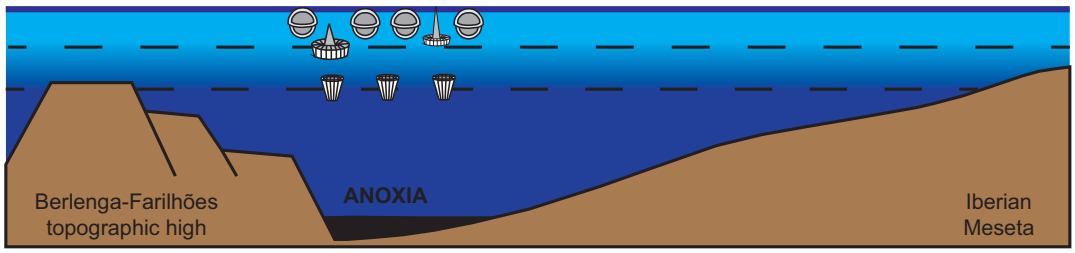

(1) Restricted basin, low sea level, reduced photic zone

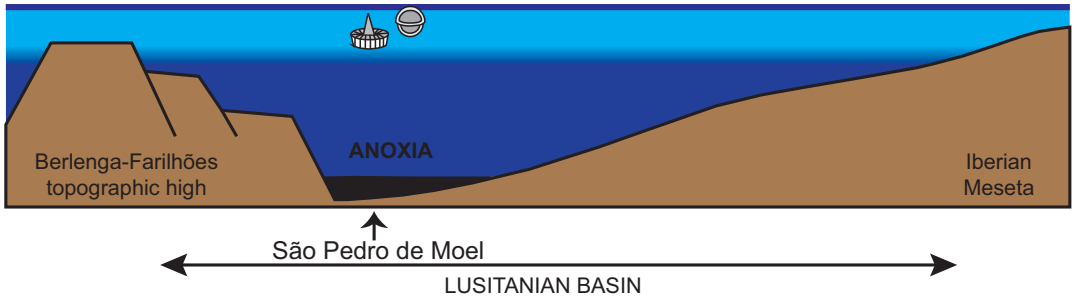

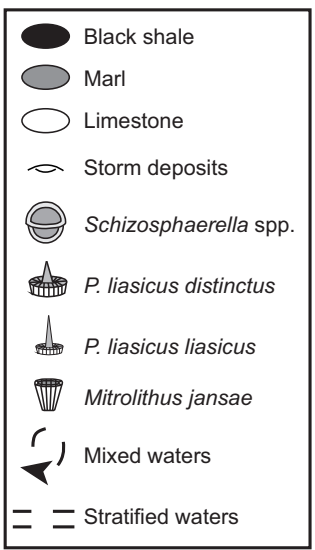

Dataset

Click here to download Background dataset for online publication only: Dataset.xlsx